

Accepted Manuscript

Effect of temporal aggregation on the estimate of annual maximum rainfall depths for the design of hydraulic infrastructure systems

Renato Morbidelli, Carla Saltalippi, Alessia Flammini, Marco Cifrodelli, Tommaso Picciafuoco, Corrado Corradini, M. Carmen Casas-Castillo, Hayley J. Fowler, Sean M. Wilkinson

PII: S0022-1694(17)30654-6
DOI: <https://doi.org/10.1016/j.jhydrol.2017.09.050>
Reference: HYDROL 22270

To appear in: *Journal of Hydrology*

Received Date: 10 March 2017
Revised Date: 26 September 2017
Accepted Date: 27 September 2017

Please cite this article as: Morbidelli, R., Saltalippi, C., Flammini, A., Cifrodelli, M., Picciafuoco, T., Corradini, C., Casas-Castillo, M.C., Fowler, H.J., Wilkinson, S.M., Effect of temporal aggregation on the estimate of annual maximum rainfall depths for the design of hydraulic infrastructure systems, *Journal of Hydrology* (2017), doi: <https://doi.org/10.1016/j.jhydrol.2017.09.050>

This is a PDF file of an unedited manuscript that has been accepted for publication. As a service to our customers we are providing this early version of the manuscript. The manuscript will undergo copyediting, typesetting, and review of the resulting proof before it is published in its final form. Please note that during the production process errors may be discovered which could affect the content, and all legal disclaimers that apply to the journal pertain.



1 **Effect of temporal aggregation on the estimate of annual maximum rainfall**
2 **depths for the design of hydraulic infrastructure systems**

3

4 Renato Morbidelli¹, Carla Saltalippi, Alessia Flammini, Marco Cifrodelli, Tommaso
5 Picciafuoco and Corrado Corradini

6

7 Dept. of Civil and Environmental Engineering, University of Perugia, via G. Duranti 93, 06125 Perugia, Italy

8

9 M. Carmen Casas-Castillo

10

11 Dept. de Física, ESEIAAT, Universitat Politècnica de Catalunya, BarcelonaTech (UPC), Terrassa, Spain

12

13 Hayley J. Fowler, Sean M. Wilkinson

14

15 School of Civil Engineering and Geosciences, Newcastle University, UK

16

17 **Abstract**

18

19 For a few decades the local rainfall measurements are generally obtained by tipping bucket
20 sensors, that allow to record each tipping time corresponding to a well-known rain depth.

21

22 However, a considerable part of rainfall data to be used in the hydrological practice is
23 available in aggregated form within constant time intervals. This can produce undesirable

24

25 effects, like the underestimation of the annual maximum rainfall depth, H_d , associated with a
26 given duration, d , that is the basic quantity in the development of rainfall depth-duration-

27

28 frequency relationships. The errors in the evaluation of H_d from data characterized by a coarse
temporal aggregation, t_a , and a procedure to reduce the non-homogeneity of the H_d series are

29

30 here investigated. Our results show that for $t_a=1$ minute the underestimation is practically
negligible, whereas for larger temporal aggregations with $d=t_a$ the error in a single H_d can

31

reach values up to 50% and in a series of H_d in the average up to 17%. Relationships between

¹ Correspondence to: R. Morbidelli, Department of Civil and Environmental Engineering, University of Perugia, Via Duranti 93, 06125 Perugia, Italy. E-mail: renato.morbidelli@unipg.it

29 the non-dimensional ratio t_a/d and the average underestimation of H_d , derived through
30 continuous rainfall data observed in many stations of Central Italy, are presented to overcome
31 this issue. These equations allow to improve the H_d estimates and the associated depth-
32 duration-frequency curves at least in areas with similar climatic conditions. The effect of the
33 correction of the H_d series on the rainfall depth-duration-frequency curves is quantified. Our
34 results indicate that the improvements obtained by the proposed procedure are of the order of
35 10%.

36
37 KEY WORDS Rainfall data, Temporal aggregation, Annual maximum rainfall depths,
38 Depth-duration-frequency curves

41 1. Introduction

42 Rainfall data with relatively high time resolution are essential for many hydrologic studies,
43 including the development of rainfall modeling (Corradini and Melone, 1989; Haile et al.,
44 2011a), simulation of infiltration (Melone et al., 2008), representation of the mechanisms of
45 runoff generation (Govindaraju et al., 1999), description of soil erosion (e.g. Angel et al.,
46 2005) and even design of hydraulic infrastructure systems (Adamowski et al., 2010; Notaro et
47 al., 2015). The last topic relies upon the determination of rainfall depth-duration-frequency
48 relationships (Willems, 2000; Overeem et al., 2008) which require the knowledge of the
49 annual maximum rainfall depths, H_d , accumulated over different durations, d (Koutsoyiannis
50 et al., 1998). The time resolution of rainfall data can play a significant role, particularly in the
51 estimation of extreme rainfalls with short duration that are of primary importance in the
52 design of widespread hydraulic and drainage infrastructure systems (Du Plessis and Burger,
53 2015).

54 Historical rainfall data may be available with different temporal aggregations (or time
55 resolutions), t_a , linked to the progress of recording systems through time. Currently, through
56 tipping bucket sensors, rainfall amounts are recorded in a data-logger for each tip time
57 associated with a fixed rainfall depth (usually 0.1 or 0.2 mm). The rain event properties are
58 then summarized by aggregating the number of tips over a selected t_a , that can vary from 1
59 minute to much longer time intervals.

60 After this aggregation procedure, rainfall analyses at temporal scales smaller than the adopted
61 t_a cannot be derived, while for $d \geq t_a$ they can be affected by significant errors (Haile et al.,
62 2011b).

63 This occurs because often in hydrological practice there is no access to basic metadata
64 collected by hydrological agencies, particularly in the case of historical data derived from
65 potentially inaccurate long-standing recording systems (e.g. paper rolls). The quantification of
66 the errors in extreme rainfall amount caused by different values of d for a fixed t_a have been
67 analyzed in several studies. It is well known that for d comparable with t_a the actual maximum
68 accumulations may be underestimated (Hershfield, 1961; Weiss, 1964; Young and McEnroe,
69 2003; Yoo et al., 2015). Hershfield (1961) observed that for $d=t_a$ the results obtained from an
70 analysis based on actual maxima were closely approximated through a frequency analysis of
71 H_d with values multiplied by 1.13. Weiss (1964), on probabilistic grounds, under the
72 assumption of a uniform rainfall throughout the duration of interest, developed a relationship
73 between the sampling ratio, t_a/d , and the average ratio of the real maximum rainfall
74 accumulation for a given d to the maximum one deduced by a fixed recording interval,
75 henceforth designated as sampling adjustment factor (SAF). Young and McEnroe (2003) used
76 high temporal resolution data from 15 rain gauges located in the Kansas City metropolitan
77 area to derive a single empirical relationship between SAF and sampling ratio. This relation
78 was found to provide adjustments consistent with other empirical studies (Miller et al., 1973;

79 Frederick et al., 1977; Huff and Angel, 1992). However, the length of the considered rainfall
80 series (in the range 5.3-14.9 years, with average value of 9.6 years) was too limited to draw a
81 conclusion of general validity. Yoo et al. (2015) extended the probabilistic approach
82 presented by Weiss (1964) considering several not uniform rainfall temporal distributions that
83 were found significantly related with the SAF. Overall, previous studies suggest that the SAF
84 is dependent on both sampling ratio and d , with the latter that is involved because the shape of
85 the rainfall temporal distribution is linked to it.

86 The first objective of this paper is to define, for a given duration, the length of a H_d series,
87 observed with a given aggregation time, that is required to derive an average adjustment
88 factor to be applied to each series element to reduce the involved original errors. Considering
89 the random nature of H_d this is an important point, but sometimes it has not been considered
90 in depth. We note, for example, that Young and McEnroe (2003) used series with fairly short
91 length and did not examine the problem of their reliability in the determination of the
92 adjustment factors. In this study we use, as a benchmark, rainfall data observed for many
93 years with an aggregation time of 1 minute. Furthermore, in the analysis performed for t_a and
94 d of interest the series incorporate rainfall temporal distributions with a variety of shapes that
95 included the different theoretical distributions supposed by Yoo et al. (2015). The second
96 objective of this paper is to define a methodology to obtain homogeneous series of annual
97 maximum rainfall depths from data derived through different temporal aggregations. This is a
98 crucial issue because many rain gauge stations were installed in the first half of the twentieth
99 century and their series of annual maximum rainfall depths are not homogeneous
100 (Alexandersson, 1986; Hanssen-Bauer and Forland, 1994) as a result of many values derived
101 from rainfall data with a coarse t_a (e.g. when a recording system on rolling paper was adopted)
102 and the remaining ones with $t_a=1$ minute. The third objective of this paper is to estimate the

103 sensitivity of the rainfall depth-duration-frequency curves to the corrections of the H_d series
 104 performed by the proposed methodology.

107 2. Methods

108 Following Burlando and Rosso (1996) and Boni et al. (2006) we provide the definition of
 109 annual maximum rainfall depth through the rainfall rate at time t , $x(t)$, measured at a specific
 110 location. The accumulated rainfall recorded over a time interval d , $x_d(t)$, is given by:

$$112 \quad x_d(t) = \int_t^{t+d} x(\xi) d\xi \quad (1)$$

113
 114 The annual maximum rainfall depth over a duration d , H_d , is therefore expressed as:

$$116 \quad H_d = \max[x_d(t) : t_0 < t < t_0 - d + 1 \text{ year}] \quad (2)$$

117
 118 where t_0 is the starting time of each year.

119 To determine H_d for a specific year, the knowledge of rainfall data characterized by any $t_a \leq d$
 120 is necessary. When $d=t_a$, independently of the rainfall pulse shape, the H_d value is sometimes
 121 correctly estimated (Fig. 1a) but can also be underestimated (Figs. 1b-c) with errors up to
 122 50% (Fig. 1c). The underestimation error adopted here is directly related to both the SAF
 123 introduced by Young and McEnroe (2003) and the correction factor of Yoo et al. (2015).

124
 125
 126 *insert here Fig. 1*

127

128

129

Despite the inability to correctly quantify the accuracy of a given H_d value, a representation of the average error for a time series containing a large number of elements can be established.

130

It is well-known that for each duration d , a long H_d series is affected by an average error

depending on both t_a and the shape of the rainfall pulses. In the case of rectangular pulses, the

average underestimation is equal to 25%, because each error assumes with the same

probability of occurrence a value in the range 0-50%. This is consistent with the theoretical

results by Yoo et al. (2015). However, it is widely recognized that the H_d values are

determined by heavy rainfalls of erratic shape (Balme et al., 2006; Al-Rawas and Valeo,

2009; Coutinho et al., 2014). For example, Fig. 2 shows a few sample hyetographs associated

with the annual maximum rainfall rates for $d=60$ minutes that were recorded by a rain gauge

station located in Central Italy. The hyetographs exhibit irregular shapes that can be roughly

considered of triangular type.

141

142

143 *insert here Fig. 2*

144

145

146 Under the assumption of a triangular rainfall pulse characterized by a duration d , the total

147 rainfall depth, R_{pd} , is (Fig. 3a):

148

$$149 \quad R_{pd} = \frac{dh}{2} \quad (3)$$

150

151 with h equal to the rainfall intensity peak.

152 When $t_a=d$, also with a triangular pulse the underestimation error of a single H_d is within the
 153 range 0-50%. The error associated with the possible pulse positions (Fig. 3b) is displayed in
 154 Fig. 3c. Its average value, E_a , obtained by integration through the pulse duration (see also Yoo
 155 et al., 2015) is given by:

156

$$157 \quad E_a = \frac{1}{12} t_a h \quad (4)$$

158

159 This quantity may be expressed in terms of percentage of the rainfall pulse depth as:

160

161

$$162 \quad E_{a\%} = 100 \frac{E_a}{R_{pd}} \quad (5)$$

163

164 For $t_a=d$, $E_{a\%}$ assumes the value 16.67% that agrees with the conclusions by Yoo et al. (2015).

165

166 *insert here Fig. 3*

167

168

169 However, an analysis of a considerable number of measured hyetographs performed for
 170 different rain gauge stations and d values highlights that in many cases before and after the

171 peak the rainfall depth exhibits a steeper trend (Fig. 4). Therefore the actual value of $E_{a\%}$

172 should be less than 16.67%.

173

174

175 *insert here Fig. 4*

176

177

178 We note that, in principle, underestimation errors in determining the H_d values cannot be
 179 eliminated, independently of the adopted t_a . Moreover, the average error $E_{a\%}$ decreases when
 180 the ratio t_a/d decreases. For example, from eqs. (3) and (5) it follows that:

181

$$182 \quad E_{a\%}(d = nt_a) = \frac{1}{n} E_{a\%}(d = t_a) \quad n = 1, 2, \dots \quad (6)$$

183

184 which implies that for t_a/d sufficiently small $E_{a\%}$ becomes negligible.

185 On the basis of the aforementioned analysis, if $d=t_a=1$ minute for an extreme rainfall event of
 186 intensity equal to 300 mm/h the underestimation error becomes less than 1 mm. Further,
 187 considering that from a practical point of view the durations of interest for H_d are always ≥ 5
 188 minutes, rainfall data with $t_a=1$ minute may be considered with negligible error as continuous
 189 data.

190

191 3. Experimental system

192 Rainfall data used in this study were mainly recorded in the Umbria Region (8456 km²),
 193 located in Central Italy. This Region is characterized by a complex orography of mountainous
 194 type along the eastern side, where the Apennine Mountains exceed 2000 m a.s.l., and of hilly
 195 type with elevation ranging from 100 to 800 m a.s.l., in the central and western areas.

196 Mean annual rainfall, for 1921-2015, is about 900 mm but varies spatially from 650 mm to
 197 1450 mm. Higher monthly rainfall values generally occur during the autumn-winter period,
 198 when floods caused by widespread rainfall are frequently observed.

199 A wide part of the study area is included in the Tiber River basin, which crosses the Region
200 from North to South-West, receiving water from many tributaries mainly located on the
201 hydrographic left side.

202 The study area is currently monitored through a dense rain gauge network (about 1 rain gauge
203 every 90 km²) mostly with a continuous ($t_a=1$ minute) connection to a central unit by a radio
204 link. Before 1992 a reduced rain gauge network (18 devices) was in operation with $t_a=30$
205 minutes.

206 In this study only the rain gauge stations characterized by continuous rainfall data for at least
207 20 years (16 out of 93), are considered. Their geographic position, together with the main
208 characteristics of the selected time series, are summarized in Fig. 5.

209 The selected rain gauge stations were divided into two groups: one with 12 stations used
210 during a first phase to develop a methodology of data analysis and the other with 4 stations
211 preserved for validation purposes.

212 Rainfall data from the Fabra Observatory of Barcelona (Spain) (Burgueño et al., 1994; Casas
213 et al., 2004), with elevation 411 m a.s.l. are also considered for the validation stage. Due to
214 the location on the northeast coast of the Iberian Peninsula, rainfall in Barcelona is rather
215 limited with an average annual depth less than 640 mm distributed in few rainy days (55 per
216 year), usually in late summer and autumn when advection of warm and humid air from the
217 Mediterranean Sea can cause heavy rainfall events of convective type (Rodríguez-Solà et al.,
218 2017). Rainfall data from Barcelona were recorded in the period 1951 – 1981 with $t_a=1$
219 minute.

220

221

222 *insert here Fig. 5*

223

224

225 **4. Results**226 *4.1 Development of average error relationship*

227 Starting from the continuous rainfall data of all selected stations, aggregated data with the
228 following t_a were obtained: 1 minute, henceforth denoted as “Observed”; 10, 15, 30, 60, 180,
229 360, 720 and 1440 minutes, henceforth denoted as “Generated”. An example of this procedure
230 is shown in Table I for rainfall data recorded at the Petrelle station.

231 For each selected station and considering some typical values of d (≤ 1440 minutes), all H_d
232 values may be easily determined by using both the “Observed” and “Generated” data. For
233 each set of rainfall data, H_d can be deduced only for $d \geq t_a$.

234

235

236 *insert here Tab. I*

237

238

239 Assuming each H_d value obtained from the observed data as a benchmark, the H_d
240 underestimation caused by the use of rainfall data with a coarse t_a (“Generated”) can be
241 quantified. As representative cases, Tables II and III highlight the underestimation errors for
242 the Bastia Umbria station considering temporal aggregations equal to 30 and 15 minutes,
243 respectively. It can be seen that, for fixed t_a and d , errors can randomly vary with years. The
244 minimum underestimation error in Table II is practically negligible (0.32% in 1992) for
245 $t_a=d=30$ minutes, whereas the error increases to about 34% in 1997. It may be observed that
246 more significant errors occur when $t_a=d$, while they become less than 1% when $t_a/d \leq 0.1$. A
247 comparison of Tables II and III shows that the error magnitude, particularly in terms of the
248 average value for all years, is mainly related to the ratio t_a/d . For example, values in the third

249 column of Table II (where $d=60$ minutes and $t_a/d=0.5$) are comparable with those in the
250 second column of Table III (where $d=30$ minutes and $t_a/d=0.5$), with a difference in terms of
251 average values less than 1%. However, Table IV shows that in some cases these differences
252 become significant because the average underestimation errors depend also on d . For equal
253 ratios of t_a/d a smaller average error is obtained when d is longer because the probability to
254 have a dry period is higher.

255

256

257 *insert here Tab. II*

258

259 *insert here Tab. III*

260

261 *insert here Tab. IV*

262

263

264 Additional information on our results are given in Fig. 6, that indicates the absence of a link
265 between the rain gauge location and the error magnitude.

266

267

268 *insert here Fig. 6*

269

270

271 Finally, the dependence of the average error on the length of the data series has been
272 investigated. Figure 7 shows the error variability with increasing the measurement period that
273 precedes the last H_d value. The results of this analysis, performed using series with a length of
274 at least 20 years, are synthesized through a few representative cases referred to $t_a/d=1$ and

275 $d \gg t_a$, which determine extreme values of the average error. From Figs. 7a-f it can be seen
276 that increasing the series dimension the average error trend is rather irregular, independently
277 of the ratio t_a/d . This is an expected result considering that H_d is a random variable. However,
278 it is possible to deduce the data series length required to obtain a reliable estimation of the
279 average error. In most cases it should be approximately greater than 15-20 years (Figs. 7a-e),
280 but for $d \gg t_a$ (Fig. 7e) the average error magnitude is of minor importance even though much
281 shorter lengths are used. These results highlight a possible critical point in the earlier study by
282 Young and McEnroe (2003) who examined data series with average length less than 10 years.
283 However, a partial support to their study is given by the results we have obtained in a limited
284 number of historical series for which a length approximately greater than 7 years (Fig. 7f)
285 seems to be appropriate for the average error estimation.

286

287

288 *insert here Fig. 7*

289

290

291 An overall analysis of our results suggests that:

- 292 – the developments presented in Sect. 2 for the evaluation of errors on H_d are
- 293 substantially well-founded;
- 294 – in any case an average error becomes reliable if its estimation is carried out on the
- 295 basis of at least 15-20 years of observed rainfall data;
- 296 – the largest average error occurs for $d=t_a$ and does not exceed 16.67%;
- 297 – for $d=nt_a$ the average error is less than or equal to $(1/n)16.67\%$;
- 298 – the average error depends on both t_a/d and d ;

- 299 – for each specific year the error is a random quantity with value in any case less than or
 300 equal to 50%;
- 301 – the average errors are independent of the considered rain gauge location.

302

303 *4.2 Correction of H_d*

304 The aforementioned results account for the effect of temporal aggregation on H_d values, either
 305 for a specific year or for a long time series. Therefore, on this basis we can define a
 306 methodology to improve the homogeneity of H_d series obtained from rainfall data with very
 307 different temporal aggregations.

308

309 Considering only rainfall data observed in the stations selected for the first phase of this work,
 310 Fig. 8 displays all average underestimation errors for different values of t_a/d , including those
 311 obtained from daily rainfall data. The best interpolation function can be expressed as:

311

$$312 \quad E_{a\%} = 4.01 \left(\frac{t_a}{d} \right)^2 + 6.94 \frac{t_a}{d} \quad [\%] \quad (7)$$

313

314 From Fig. 8 it can be deduced the uncertainty associated to the results obtained by eq. (7).

315 This should be useful in hydrological practice because the users could decide, particularly for

316 $t_a/d=1$, which estimation to adopt depending on the level of risk they want to assume.

317

318

319 *insert here Fig. 8*

320

321

322 Furthermore, Fig. 8 shows that our results are very close to those obtained by Young and
323 McEnroe (2003) even though, as above discussed, in general terms they considered too short
324 series of H_d with lengths in the range 5.3-14.9 years while lengths larger than 15-20 years
325 could be in principle more appropriate considering also the random nature of the investigated
326 variable. The reliable curve of Fig. 8 obtained by Young and McEnroe (2003) could be
327 therefore ascribed to a use, for $t_a/d=1$, of a significant number of series with lengths close to
328 15 years and to stations with rainfall temporal structure similar to that characterizing our
329 representative station of Fig. 6f. In any case, the stations to implement to obtain acceptable
330 data corrections through shorter series lengths cannot be identified a priori, therefore the good
331 relation proposed by Young and McEnroe (2003) does not justify the adoption of series with
332 too short duration. In addition, Fig. 8 highlights a significant difference between our
333 representation of the average error by eq. (7) and that proposed by Weiss (1964), who in his
334 probabilistic approach assumed a uniform rainfall rate through the accumulation period. In the
335 light of our analysis on the rainfall patterns observed in the study stations, this assumption
336 does not appear fully justified even though the adjustment factor was applied as an average
337 quantity to the series of annual maximum rainfall depths with a given duration. From our
338 experimental data we deduced that the assessment of $E_{a\%}$ could be further improved by
339 splitting eq. (7) on the basis of the duration of interest because of its link with the shape of the
340 rainfall temporal distribution that influences the error magnitude (Yoo et al., 2015).
341 Rectangular rainfall pulses were typically observed for d up to 30 minutes, triangular pulses
342 for greater values of d up to 180 minutes and pulses representable by quadratic functions
343 (Yoo et al., 2015) for larger values of d . On this basis the following three relations, plotted in
344 Fig. 9, were derived:

345

$$346 \quad E_{a\%} = 6.14 \left(\frac{t_a}{d} \right)^2 + 5.96 \frac{t_a}{d} \quad [\%] \quad d \leq 30 \text{ minutes}$$

$$347 \quad E_{a\%} = 6.7 \left(\frac{t_a}{d} \right)^2 + 4.72 \frac{t_a}{d} \quad [\%] \quad 30 \text{ minutes} < d < 180 \text{ minutes} \quad (8)$$

$$348 \quad E_{a\%} = 5.2 \left(\frac{t_a}{d} \right)^2 + 5.57 \frac{t_a}{d} \quad [\%] \quad d \geq 180 \text{ minutes}$$

349

350

351 *insert here Fig. 9*

352

353

354

355

356

357

358

359

360

361

362

363

364

365

366

367 *insert here Fig. 10*

368

For each value of t_a/d and d , eq. (8) can be used to quantify the correction to be apply to the H_d series obtained from data with a coarse t_a . Through a sensitivity analysis it was checked that the number of stations adopted was sufficiently high to assure the robustness of the proposed methodology. This methodology was validated using rainfall data from the 2nd group of stations located in the study area and from the Barcelona station (Burgueño et al., 1994). Each series of H_d values obtained with coarse t_a (10, 15, 30, ... minutes) was corrected by adding the quantity given by eq. (8) and then compared with the “Observed” series ($t_a=1$ minute). Figure 10 shows the corrected average H_d values, for all the examined combinations of t_a and d , against the benchmark values obtained from the rainfall data characterized by $t_a=1$ minute. The proposed methodology provides an accurate representation of the actual average H_d values, with determination coefficients in respect to the bisecting line higher than 0.99.

369
370
371
372
373
374
375
376
377
378
379
380
381
382
383
384
385
386
387
388
389
390
391
392
393

The improvements obtained through the application of the developed methodology can also be deduced from Table V, where positive and negative values of the residual average error after the correction by eq. (8) indicate underestimation and overestimation, respectively, and from Fig. 11, referred to cases with $t_a/d=1$. In many cases the residual average errors become of minor interest.

insert here Tab. V

insert here Fig. 11

Finally, the effect of the correction of H_d on the rainfall depth-duration frequency curves was quantified. This issue is addressed below through the description of both the adopted procedure and the results obtained for the representative rain gauge station of Gubbio. For each duration, in addition to 24 values of H_d appropriately observed with $t_a=1$ minute (see also Fig. 5), 20 values obtained from data recorded earlier than 1992 with $t_a=30$ minutes were used. This H_d series represents the uncorrected one, while a series including the 24 values of H_d observed with $t_a=1$ minute and the remaining 20 values modified by the proposed methodology is denoted as the corrected series. The statistical analysis of each random variable, H_d , was performed using the Generalized Extreme Value (Jenkinson, 1955; Coles, 2001) distribution function. Figure 12 indicates that for durations up to 3 h the error expressed as a percentage of the annual maximum rainfall depth is slightly variable with both return period and duration and that the use of uncorrected H_d series determines depth underestimations between 5% and 10%. Similar results were obtained for durations up to 24

394 h. Furthermore, we note that the above errors would experience an appreciable increase in the
395 case the uncorrected series involving only data deduced through $t_a \gg 1$ minute.

396

397 *insert here Fig. 12*

398

399

400

401 **5. Conclusions**

402 The evaluation of rainfall depth-duration-frequency curves should be made by using H_d
403 values derived from continuously recorded rainfall depths but until few decades ago these
404 were available only with coarse temporal aggregations. Therefore, a correction of the H_d
405 values deduced from data recorded with a significant temporal aggregation is required for
406 hydrological applications.

407 In this paper we have first examined in depth a few critical points already remarked in
408 previous works. Our study, developed through the use of a large number of rain gauge
409 stations operative for many years with $t_a=1$ minute, emphasizes the following elements:

- 410 – H_d values derived from rainfall data characterized by every t_a involves underestimation
411 errors, that for $t_a \gtrsim 10$ minutes can become important;
- 412 – in the worst conditions, that occur for $d=t_a$, a single H_d value can be affected by an
413 underestimation error up to 50%, while the average underestimation error for a series
414 of appropriate length is less than or equal to 16.7%;
- 415 – each H_d series usually contains many values significantly underestimated. In our study
416 area, equipped with 93 rain gauge stations, the percentage of H_d values determined by
417 rainfall data recorded with $t_a \geq 30$ minutes is equal to 34.7%, with a value of 100% for a
418 few series.

419 On this basis we have shown that:

- 420 – to develop reliable relationships between the average underestimation error, $E_{a\%}$, and
- 421 values of t_a and d , data series with a length of at least 15-20 years have to be available;
- 422 – a relationship between $E_{a\%}$ and t_a/d split up into three expressions associated with
- 423 different duration ranges enables us to obtain very reliable H_d series;
- 424 – the use of uncorrected H_d series for the determination of rainfall depth-duration-
- 425 frequency curves can lead to underestimations of the order of 10%.

426

427

428

429 **Acknowledgment**

430 The authors are thankful to the Umbria Region and its Functional Centre for providing the
431 rainfall data and I. Bavicchi, L. Pesaresi and M. Stelluti for their technical assistance.

432 This research was mainly financed by the Italian Ministry of Education, University and
433 Research (PRIN 2015). It also forms part of the INTENSE project through the European
434 Research Council (grant ERC-2013-CoG-617329). Hayley Fowler is funded by the Wolfson
435 Foundation and the Royal Society as a Royal Society Wolfson Research Merit Award
436 (WM140025) holder.

437

438

439

440 **References**

441 Adamowski J, Adamowski K, Bougadis J. 2010. Influence of trend on short duration design
442 storms. *Water Resour. Manage.*, 24, 401-413.

443 Alexandersson H. 1986. A homogeneity test applied to precipitation data. *J Climatol.*, 6(6),
444 661-675.

- 445 Al-Rawas GA, Valeo C. 2009. Characteristics of rainstorm temporal distributions in arid
446 mountainous and coastal regions. *J. Hydrol.*, 376(1-2), 318-326.
- 447 Angel JR, Palecki MA, Hollinger SE. 2005. Storm precipitation in the United States, Part II:
448 soil erosion characteristics. *J. Appl. Meteorol.*, 44(6), 947-959.
- 449 Balme M, Vischel T, Lebel T, Peugeot C, Galle S. 2006. Assessing the water balance in the
450 Sahel: Impact of small scale rainfall variability on runoff, Part 1: Rainfall variability
451 analysis. *J. Hydrol.*, 331(1-2), 336-348.
- 452 Boni G, Parodi A, Rudari R. 2006. Extreme rainfall events: Learning from raingauge time
453 series. *J. Hydrol.*, 327(3-4), 304-314.
- 454 Burgueño A, Codina B, Redaño A, Lorente J. 1994. Basic statistical characteristics of hourly
455 rainfall amounts in Barcelona. *Theor. Appl. Climatol.*, 49(3), 175-181.
- 456 Burlando P, Rosso R. 1996. Scaling and multiscaling models of depth-duration-frequency
457 curves for storm precipitation. *J. Hydrol.*, 187(1-2), 45-64.
- 458 Casas M. C., Codina B., Redaño A., Lorente J. 2004. A methodology to classify extreme
459 rainfall events in the western Mediterranean area. *Theor. Appl. Climatol.*, 77(3-4), 139-
460 150.
- 461 Coles S. 2001. An introduction to statistical modelling of extreme value. Springer, London.
- 462 Corradini C, Melone F. 1989. Spatial structure of rainfall an mid-latitude cold front system. *J.*
463 *Hydrol.*, 105(3-4), 297-316.
- 464 Coutinho JV, Almeida CDN, Leal AMF, Barbosa LR. 2014. Characterization of sub-daily
465 rainfall properties in three rainfall gauges located in Northeast of Brazil. *Evolving Water*
466 *Resources Systems: Understanding, Predicting and Managing Water-Society Interactions.*
467 *Proc of ICWRS2014, Bologna, Italy, June 2014, IAHS Publ. 364, 345-350.*

- 468 Du Plessis JA, Burger GJ. 2015. Investigation into increasing short-duration rainfall
469 intensities in South Africa, *Water SA*, 41(3), 416-424.
- 470 Frederick RH, Myers VA, Auciello EP. 1977. Five-to 60-minute precipitation frequency for
471 the eastern and central United States. NOAA Technical Memorandum NWS HYDRO-35.
472 National Oceanic and Atmospheric Administration, National Weather Service, Silver
473 Spring, MD.
- 474 Govindaraju RS, Morbidelli R, Corradini C. 1999. Use of similarity profiles for computing
475 surface runoff over small watersheds, *J. Hydrol. Eng.*, 4(2), 100-107.
- 476 Haile AT, Rientjes THM, Gieske A, Jetten V, Mekonnen G. 2011a. Satellite remote sensing
477 and conceptual cloud modelling for convective rainfall simulation. *Adv. Water Resour.*,
478 34(1), 26-37.
- 479 Haile AT, Rientjes THM, Habib E, Jetten V, Gebremichael M. 2011b. Rain event properties
480 at the source of the Blue Nile River. *Hydrol. Earth Syst. Sci.*, 15(3), 1023-1034.
- 481 Hanssen-Bauer I, Forland EJ. 1994. Homogenizing long Norwegian precipitation series. *J.*
482 *Clim.*, 7(6), 1001-1013.
- 483 Hershfield DM. 1961. Rainfall frequency atlas of the United States for durations from 30
484 minutes to 24 hours and return periods from 1 to 100 years. US Weather Bureau Technical
485 Paper N. 40, U.S. Dept. of Commerce, Washington, DC.
- 486 Huff FA, Angel JR. 1992. Rainfall frequency atlas of the Midwest. Illinois State Water
487 Survey Bulletin 71, Midwest Climate Center Research Rep. 92-03, Illinois State Water
488 Survey, Champaign, IL.
- 489 Jenkinson AF. 1955. The frequency distribution of the annual maximum (or minimum) values
490 of meteorological elements. *Q. J. R. Meteorol. Soc.*, 81(348), 158-171.

- 491 Koutsoyiannis D, Kozonis D, Manetas A. 1998. A mathematical framework for studying
492 rainfall intensity-duration-frequency relationships. *J. Hydrol.*, 206(1-2), 118-135.
- 493 Melone F, Corradini C, Morbidelli R, Saltalippi C, Flammini A. 2008. Comparison of
494 theoretical and experimental soil moisture profiles under complex rainfall patterns, *J.*
495 *Hydrol. Eng.*, 13(12), 1170-1176.
- 496 Miller JF, Frederick RH, Tracey RJ. 1973. Precipitation-frequency atlas of the western United
497 States. NOAA Atlas 2, National Weather Service, National Oceanic and Atmospheric
498 Administration, U.S. Dept. of Commerce, Washington, DC.
- 499 Notaro V, Liuzzo L, Freni G, La Loggia G. 2015. Uncertainty analysis in the evaluation of
500 extreme rainfall trends and its implications on urban drainage system design. *Water*, 7,
501 6931-6945.
- 502 Overeem A, Buishand A, Holleman I. 2008. Rainfall depth-duration-frequency curves and
503 their uncertainties. *J. Hydrol.*, 348(1-2), 124-134.
- 504 Rodríguez-Solà, R., Casas-Castillo, M. C., Navarro, X., Redaño, A. 2017. A study of the
505 scaling properties of rainfall in Spain and its appropriateness to generate intensity-
506 duration-frequency curves from daily records. *Int. J. Climatol.*, 37(2), 770-780.
- 507 Weiss LL. 1964. Ratio of true to fixed-interval maximum rainfall. *J. Hydraul. Div., Am. Soc.*
508 *Civ. Eng.*, 90(1), 77-82.
- 509 Willems P. 2000. Compound intensity/duration/frequency-relationships of extreme
510 precipitation for two seasons and two storm types. *J. Hydrol.*, 233(1-4), 189-205.
- 511 Yoo C, Jun C, Park C. 2015. Effect of rainfall temporal distribution on the conversion factor
512 to convert the fixed-interval into true-interval rainfall. *J. Hydrol. Eng.*, 20(10), 04015018.

513 Young CB, McEnroe BM. 2003. Sampling adjustment factors for rainfall recorded at fixed
514 time intervals, J. Hydrol. Eng., 8(5), 294-296.

515

516

517

ACCEPTED MANUSCRIPT

518 **List of Tables**

519

520

521 Table I – “Observed” and “Generated” rainfall data characterized by different temporal
522 aggregations, t_a , starting from January 1, 2006 at 0:00 a.m. at the Petrelle station (Umbria
523 Region, Central Italy).

524

525 Table II – Underestimation errors (in %) in the evaluation of the annual maximum rainfall
526 depth considering rainfall data with time of aggregation of 30 minutes and different durations,
527 d , at the Bastia Umbra station (Umbria Region, Central Italy).

528

529 Table III – Underestimation errors (in %) in the evaluation of the annual maximum rainfall
530 depth considering rainfall data with time of aggregation of 15 minutes and different durations,
531 d , at the Bastia Umbra station (Umbria Region, Central Italy).

532

533 Table IV – Average underestimation errors (in %) in the evaluation of the annual maximum
534 rainfall depth for the rainfall stations used during the first phase of this work. Different values
535 of duration, d , are considered. The symbol t_a denotes the aggregation time. In the last line the
536 average values representative of each duration are shown.

537

538

539 Tab. V – Errors (in %) associated with the determination of the average annual maximum
540 rainfall depth from data with aggregation time of 30 minutes for two different durations, d .
541 Rainfall data from the stations used in the validation phase. Positive and negative values
542 represent underestimation and overestimation, respectively. “Uncorrected” and “Corrected”
stand for the errors before and after the application of the proposed procedure, respectively.

543

544

545

546

547 **Figure Captions**

548

549 Fig. 1 – Schematic representation of a rectangular rainfall pulse with duration, d , equal to the
 550 measurement aggregation time, t_a : (a) condition where a correct evaluation of the annual
 551 maximum rainfall rate of duration d , H_d , is possible; (b) condition for a generic
 552 underestimation of H_d ; (c) condition for the maximum underestimation of H_d (equal to 50%).

553

554 Fig. 2 – Sample hyetographs recorded at the Bastardo station (Umbria Region, Central Italy)
 555 involving annual maximum rainfall depths for $d=60$ minutes. From top to bottom, moving
 556 windows starting on October 18, 2007 (2:17 p.m.), July 23, 2008 (4:28 a.m.) and June 26,
 557 2009 (3:10 p.m.).

558

559 Fig. 3 – Error in the evaluation of the annual maximum rainfall depth of duration d in the case
 560 of a triangular rainfall pulse and d equal to the measurement aggregation time, t_a : (a) rainfall
 561 pulse details; (b) different rainfall pulse positions and (c) corresponding errors.

562

563 Fig. 4 – Sample hyetograph recorded at the Bastardo station (Umbria Region, Central Italy)
 564 producing an annual maximum rainfall depth of duration equal to 180 minutes in 2008.
 565 Temporal window starting on July 23, 2008 (4:18 a.m.). A dashed line representing the
 566 approximate temporal behavior of the rainfall pulse is also shown.

567

568 Fig. 5 – Main characteristics of the rain gauge network selected to develop the methodology
 569 for the correction of the annual maximum rainfall depth. The geographic position is in
 570 Universal Transvers Mercator (UTM) coordinates determined by the WGS84 ellipsoid model.
 571 All the stations are in operation in the Umbria Region (Central Italy).

572

573 Fig. 6 – Average underestimation error of the annual maximum rainfall depth as a function of
 574 the aggregation time, t_a , for two different durations: (a) $d=30$ minutes; (b) $d=60$ minutes.
 575 Rainfall stations used during the first phase of this work.

576

577 Fig. 7 – Average errors in the evaluation of annual maximum rainfall depth, H_d , as a function
 578 of the number of years preceding the last H_d value for different combinations of aggregation
 579 time, t_a (in minutes), and duration, d (in minutes): (a) Bastardo station, $t_a=30$, $d=30$; (b)
 580 Cerbara station, $t_a=30$, $d=30$; (c) Ponte Santa Maria station, $t_a=60$, $d=60$; (d) Ripalvella
 581 station, $t_a=60$, $d=60$; (e) Nocera Umbra station, $t_a=30$, $d=180$; (f) Nocera Umbra station, $t_a=30$,
 582 $d=30$.

583

584 Fig. 8 – Average underestimation error of the annual maximum rainfall depth (\diamond) as a
 585 function of the ratio between temporal aggregation, t_a , and duration, d , for 12 rainfall stations
 586 used in the first phase of this work and all the combinations of t_a and d examined here. The
 587 best interpolating function together with the relations suggested by Weiss (1964) and Young
 588 and McEnroe (2003) are also plotted.

589

590

591 Fig. 9 - Average underestimation error of the annual maximum rainfall depth obtained by eq.
592 (8) as a function of the ratio between aggregation time, t_a , and duration, d .

593

594 Fig. 10 – “Corrected” average annual maximum rainfall depths, $\mu(H_d)^c$, as a function of the
595 corresponding values derived from rainfall data with $t_a=1$ minute, $\mu(H_d)^{t_a=1}$. Results from rain
596 gauge stations selected for the validation phase.

597

598

599 Fig. 11 – Average annual maximum rainfall depths, $\mu(H_d)$, versus the corresponding values
600 derived from rainfall data with $t_a=1$ minute, $\mu(H_d)^{t_a=1}$. “Uncorrected” and “Corrected” stand
601 for the values obtained before and after the application of the proposed methodology,
602 respectively. Rainfall data from the stations used in the validation phase. Only cases with
603 duration equal to the aggregation time are shown.

604

605

606 Fig. 12 – Rainfall depth-duration curves for different return periods, T_r . Comparison of curves
607 obtained by uncorrected H_d series and corresponding series corrected by the proposed
608 methodology. Sample rain gauge station of Gubbio.

609

610

611

612

613
614
615
616
617
618

Table I – “Observed” and “Generated” rainfall data characterized by different temporal aggregations, t_a , starting from January 1, 2006 at 0:00 a.m. at the Petrelle station (Umbria Region, Central Italy).

“Observed” rainfall depth (mm)	“Generated” rainfall depth (mm)							
	t_a							
I'	$10'$	$15'$	$30'$	$60'$	$180'$	$360'$	$720'$	$1440'$
0.0	0.6	0.6	0.7	2.2	12.8	20.5	23.8	32.1
0.1	0.1	0.1	1.5	4.8	7.7	3.3	8.3	2.6
0.1	0.0	0.6	1.3	5.8	2.7	7.1	0.1	5.5
0.1	0.2	0.9	3.5	6.7	0.6	1.2	2.5	0.0
0.1	0.5	0.4	3.9	0.8	5.9	0.1	5.5	0.0
0.1	0.8	0.9	1.9	0.2	1.2	0.0	0.0	0.0
0.1	0.2	1.2	5.7	0.2	1.1	0.0	0.0	0.0
0.0	0.5	2.3	1.0	1.9	0.1	2.5	0.0	0.0
0.0	0.6	2.2	0.6	0.6	0.1	5.2	0.0	0.0
0.0	0.6	1.7	0.2	0.2	0.0	0.3	0.0	0.0
0.0	1.3	0.8	0.1	0.1	0.0	0.0	0.0	0.0
0.0	1.6	1.1	0.1	0.3	0.0	0.0	0.0	0.0
0.0	1.7	2.6	0.1	0.9	0.0	0.0	0.0	0.0
0.0	1.4	3.1	0.1	1.1	0.0	0.0	0.0	0.0
0.0	0.8	0.4	1.8	3.9	0.0	0.0	0.0	0.0
0.0	0.5	0.6	0.1	0.2	2.5	0.0	0.0	0.1
0.0	0.7	0.5	0.3	0.4	4.7	0.0	0.0	0.2
0.1	0.7	0.1	0.3	0.6	0.5	0.0	0.0	0.9
0.0	1.2	0.1	0.1	0.6	0.3	0.0	0.0	0.0
0.0	2.3	0.1	0.1	0.3	0.0	0.0	0.0	0.0

619
620
621
622

623

624 Table II – Underestimation errors (in %) in the evaluation of the annual maximum rainfall
 625 depth considering rainfall data with time of aggregation of 30 minutes and different durations,
 626 d , at the Bastia Umbra station (Umbria Region, Central Italy).

<i>year</i>	<i>d (minutes)</i>					
	<i>30</i>	<i>60</i>	<i>180</i>	<i>360</i>	<i>720</i>	<i>1440</i>
1992	0.32	0	0.41	0	0	0
1993	16.22	2.22	1.54	0.02	0.89	0.08
1994	0.76	1.26	0	0	0.03	0.03
1995	23.72	3.07	3.61	0.05	0	0
1996	9.70	8.85	0	1.48	0.81	0.02
1997	34.23	0.62	6.89	0.84	0	0
1998	30.32	5.28	2.54	0.99	0.29	0.02
1999	5.02	5.26	0	0	0	0
2000	10.95	4.90	0	0.08	0.21	0
2001	1.13	0	0.66	0	0	0
2002	7.51	12.79	1.67	1.17	0.53	0
2003	21.12	7.21	1.17	0.02	0	0
2004	11.27	4.95	0.17	0.24	0	0
2005	9.66	14.76	1.44	0.02	0.73	0
2006	14.09	7.70	0.51	4.19	0.01	0
2007	21.77	1.19	1.75	0.06	0.03	0.17
2008	2.21	4.14	4.94	0	0	0.09
2009	12.18	0.61	0.67	0	0	0
2010	5.16	0	0	0	2.03	0
2012	8.62	0	0	0	2.86	0.99
2013	1.55	1.14	0.18	0	0.18	0.13
2014	14.61	9.86	2.71	0.89	0	0.12
2015	3.95	21.74	1.60	0	0	0
<i>average</i>	11.57	5.11	1.41	0.44	0.37	0.07

627

628

629

630

631 Table III – Underestimation errors (in %) in the evaluation of the annual maximum rainfall
 632 depth considering rainfall data with time of aggregation of 15 minutes and different durations,
 633 d , at the Bastia Umbra station (Umbria Region, Central Italy).

<i>year</i>	<i>d (minutes)</i>					
	<i>30</i>	<i>60</i>	<i>180</i>	<i>360</i>	<i>720</i>	<i>1440</i>
1992	0.32	0	0.41	0	0	0
1993	4.27	2.22	0.09	0.02	0.89	0.03
1994	0.76	1.26	0	0	0.03	0.03
1995	0.99	3.07	3.61	0.05	0	0
1996	1.39	0.33	0	0	0.27	0.02
1997	6.64	0.62	0.33	0.84	0	0
1998	5.16	5.03	0.58	0.46	0.01	0
1999	5.02	5.26	0	0	0	0
2000	10.95	0.63	0	0.08	0.14	0
2001	1.13	0	0.13	0	0	0
2002	7.51	9.66	0	0.86	0.53	0
2003	0.41	1.03	1.17	0.02	0	0
2004	0.12	3.69	0.03	0.03	0	0
2005	9.66	1.56	1.44	0.02	0.73	0
2006	6.19	0	0.31	1.70	0.01	0
2007	5.44	1.19	0.45	0.06	0.03	0.17
2008	2.21	0.45	4.94	0	0	0.09
2009	12.18	0.61	0.07	0	0	0
2010	5.16	0	0	0	0	0
2012	8.62	0	0	0	1.15	0.44
2013	1.55	1.14	0	0	0.18	0.13
2014	1.37	0.35	1.81	0.89	0	0.12
2015	0	0	0.53	0	0	0
<i>average</i>	4.22	1.66	0.69	0.22	0.17	0.04

634

635

636

637 Table IV – Average underestimation errors (in %) in the evaluation of the annual maximum
 638 rainfall depth for the rainfall stations used during the first phase of this work. Different values
 639 of duration, d , are considered. The symbol t_a denotes the aggregation time. In the last line the
 640 average values representative of each duration are shown.

<i>Rain gauge station</i>	<i>d (minutes)</i>					
	<i>30</i>	<i>60</i>	<i>180</i>	<i>360</i>	<i>720</i>	<i>1440</i>
	$t_a/d=1$					
Bastardo	12.47	8.28	8.39	12.70	10.14	12.71
Bastia Umbra	11.57	13.30	13.95	12.70	11.74	7.50
Casa Castalda	12.81	8.72	10.00	15.26	12.05	11.13
Cerbara	13.18	10.61	10.93	10.49	10.47	11.11
Compignano	11.13	15.58	12.99	9.06	13.58	9.00
Forsivo	12.83	10.68	7.66	4.19	8.53	12.28
Gubbio	8.50	7.15	8.41	10.91	11.65	8.29
Montelovesco	14.25	13.98	9.00	6.70	9.14	10.63
Nocera Umbra	12.73	10.26	11.97	11.57	10.72	10.97
Petrelle	15.45	11.45	14.03	12.11	10.31	12.03
Ripalvella	10.74	12.77	13.11	14.03	11.26	10.87
San Silvestro	9.64	13.10	8.76	10.04	8.66	8.70
	12.11	11.32	10.77	10.81	10.69	10.43

641

642

643

644

645

646

647

648

649

650

Tab. V – Errors (in %) associated with the determination of the average annual maximum rainfall depth from data with aggregation time of 30 minutes for two different durations, d . Rainfall data from the stations used in the validation phase. Positive and negative values represent underestimation and overestimation, respectively. “Uncorrected” and “Corrected” stand for the errors before and after the application of the proposed procedure, respectively.

<i>Rain gauge station</i>	<i>“Uncorrected”</i>		<i>“Corrected”</i>	
	<i>d=30 min</i>	<i>d=60 min</i>	<i>d=30 min</i>	<i>d=60 min</i>
Monte Cucco	9.33	6.44	-2.81	3.29
Narni Scalo	11.81	6.02	0.61	2.18
Ponte Santa Maria	17.16	5.96	5.15	2.78
San Biagio della Valle	14.08	3.74	1.75	-0.21
Barcelona (Spain)	15.85	3.34	6.40	-0.13

651

652

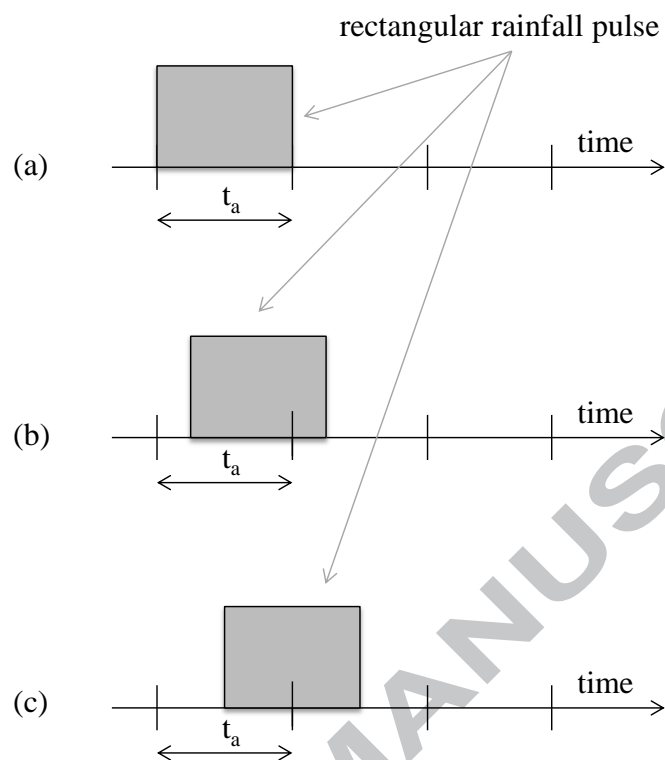


Fig. 1 – Schematic representation of a rectangular rainfall pulse with duration, d , equal to the measurement aggregation time, t_a : (a) condition where a correct evaluation of the annual maximum rainfall rate of duration d , H_d , is possible; (b) condition for a generic underestimation of H_d ; (c) condition for the maximum underestimation of H_d (equal to 50%).

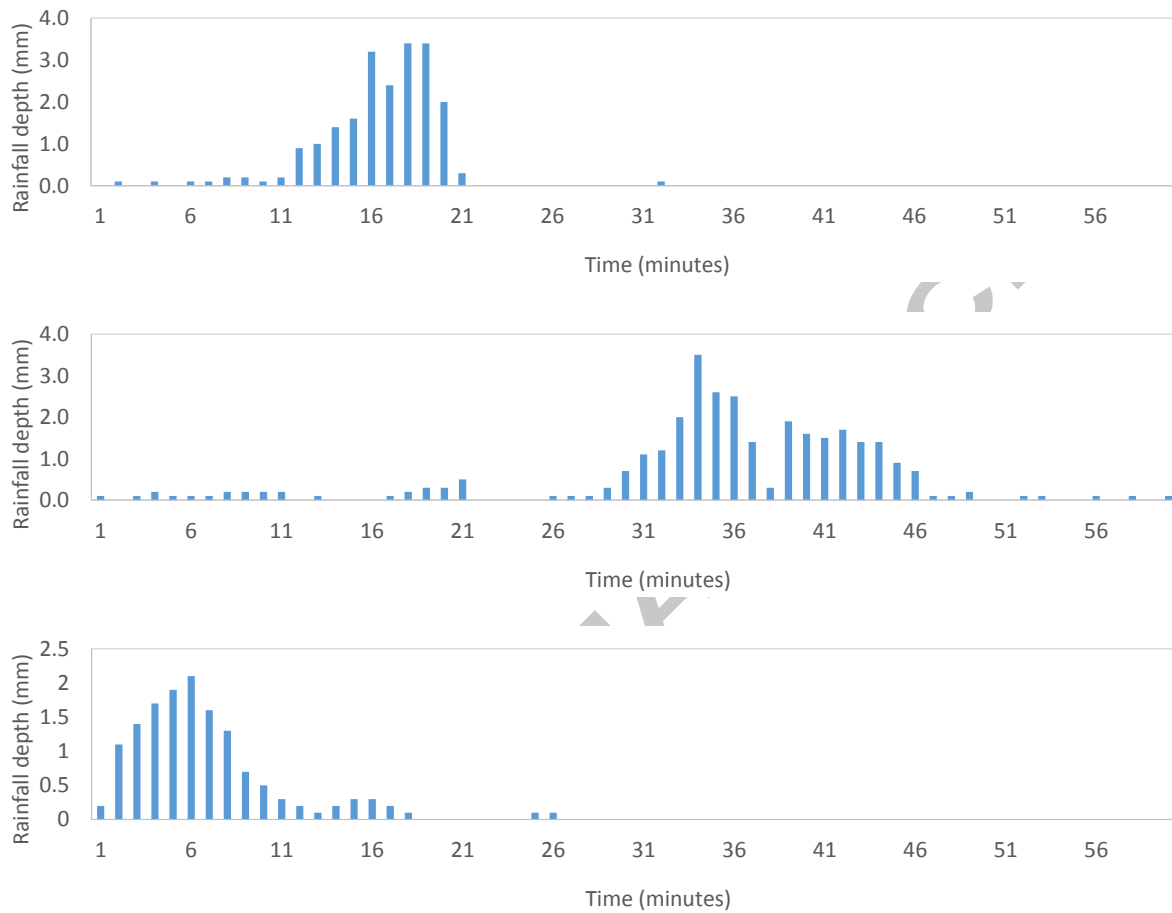


Fig. 2 – Sample hyetographs recorded at the Bastardo station (Umbria Region, Central Italy) involving annual maximum rainfall depths for $d=60$ minutes. From top to bottom, moving windows starting on October 18, 2007 (2:17 p.m.), July 23, 2008 (4:28 a.m.) and June 26, 2009 (3:10 p.m.).

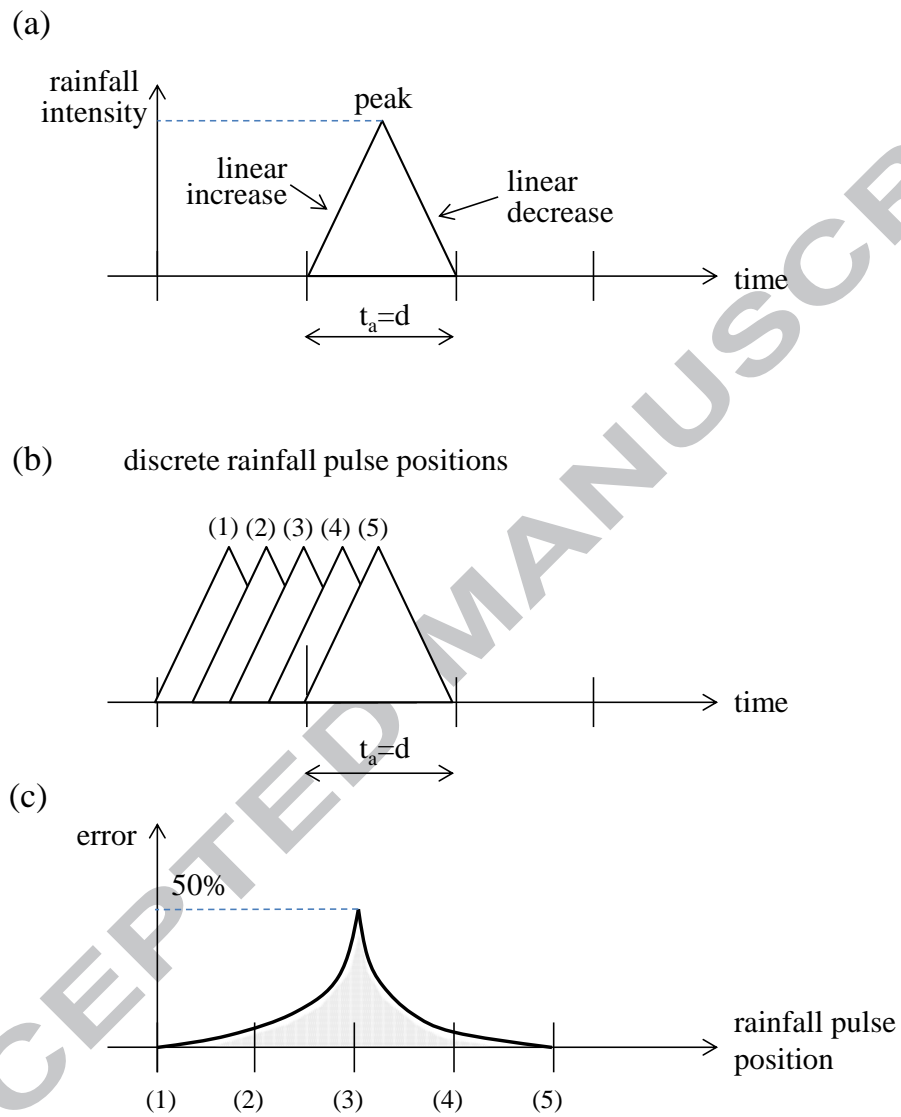


Fig. 3 – Error in the evaluation of the annual maximum rainfall depth of duration d in the case of a triangular rainfall pulse and d equal to the measurement aggregation time, t_a : (a) rainfall pulse details; (b) different rainfall pulse positions and (c) corresponding errors.

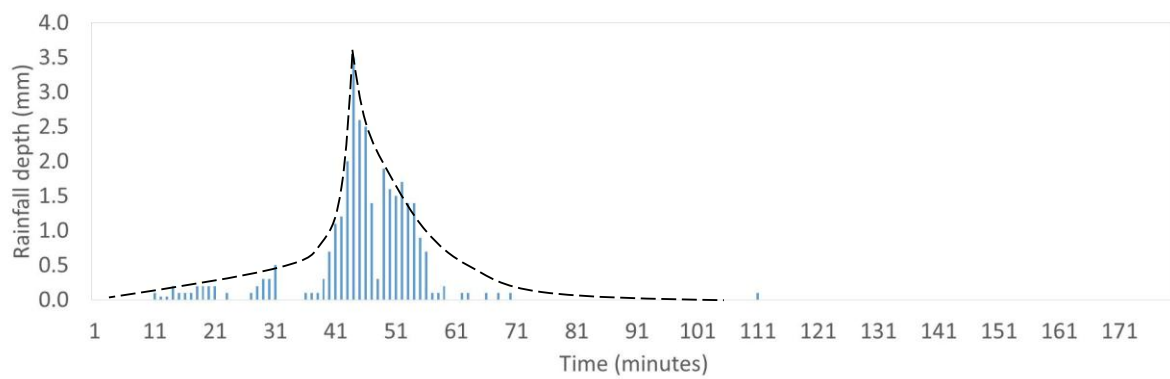
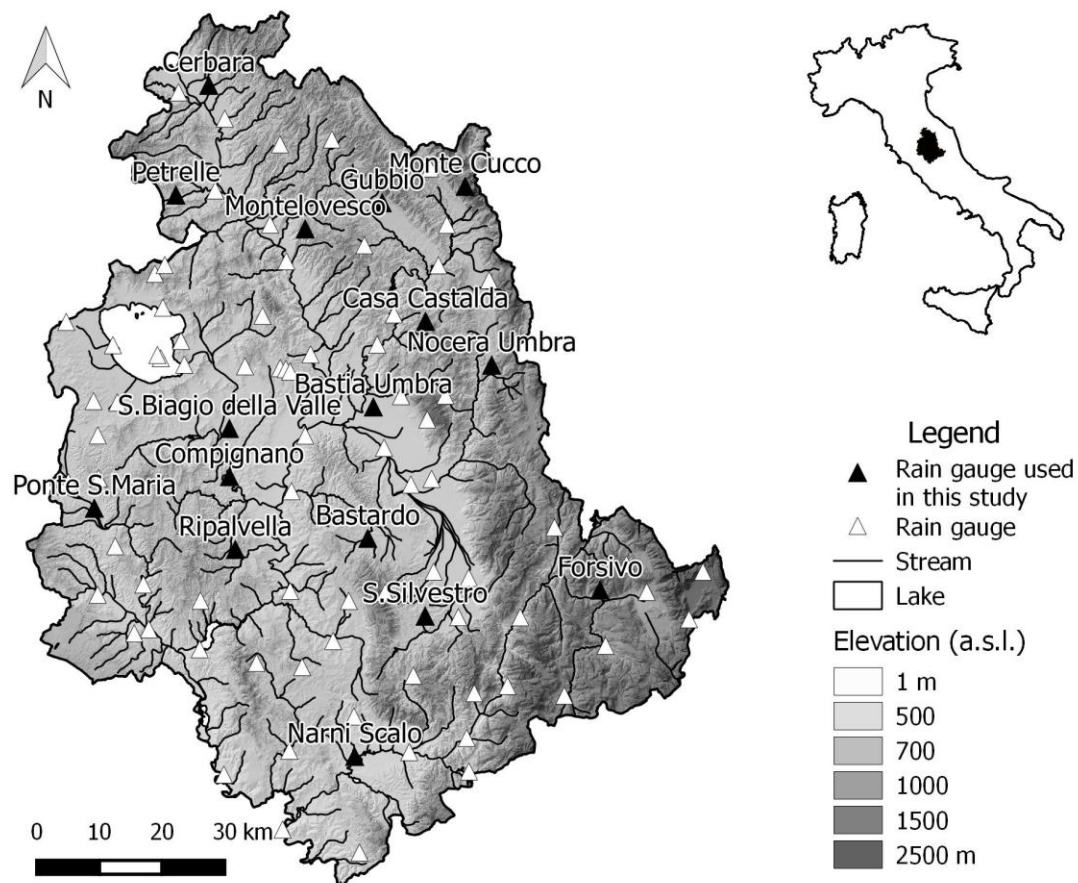


Fig. 4 – Sample hyetograph recorded at the Bastardo station (Umbria Region, Central Italy) producing an annual maximum rainfall depth of duration equal to 180 minutes in 2008. Temporal window starting on July 23, 2008 (4:18 a.m.). A dashed line representing the approximate temporal behavior of the rainfall pulse is also shown.



Raingauge station	Altitude (m a.s.l.)	UTM33 X (m)	UTM33 Y (m)	Mean annual rainfall (mm)	Available data period
<i>Bastardo</i>	331	300489	4748742	803.8	1992-2015
<i>Bastia Umbra</i>	203	301377	4769716	753.0	1992-2015
<i>Cerbara</i>	310	275092	4821081	834.3	1992-2015
<i>Casa Castalda</i>	730	309715	4783398	971.0	1992-2015
<i>Compignano</i>	240	278394	4758593	756.8	1992-2015
<i>Forsivo</i>	963	337588	4740488	867.0	1992-2015
<i>Gubbio</i>	471	302789	4802329	946.5	1992-2015
<i>Monte Cucco</i>	1087	316046	4804934	1344.4	1996-2015
<i>Montelovesco</i>	634	290484	4798142	833.0	1992-2015
<i>Narni Scalo</i>	109	298381	4713916	907.5	1992-2015
<i>Nocera Umbra</i>	534	320281	4776405	937.6	1992-2015
<i>Petrelle</i>	342	269830	4803553	897.7	1992-2015
<i>Ponte Santa Maria</i>	240	256802	4753550	790.1	1992-2015
<i>Ripalvella</i>	453	279329	4746964	879.1	1992-2015
<i>San Biagio della Valle</i>	257	278380	4766281	707.2	1993-2015
<i>San Silvestro</i>	381	309649	4736325	897.9	1992-2015

Fig. 5 – Main characteristics of the rain gauge network selected to develop the methodology for the correction of the annual maximum rainfall depth. The geographic position is in Universal Transvers Mercator (UTM) coordinates determined by the WGS84 ellipsoid model. All the stations are in operation in the Umbria Region (Central Italy).

ACCEPTED MANUSCRIPT

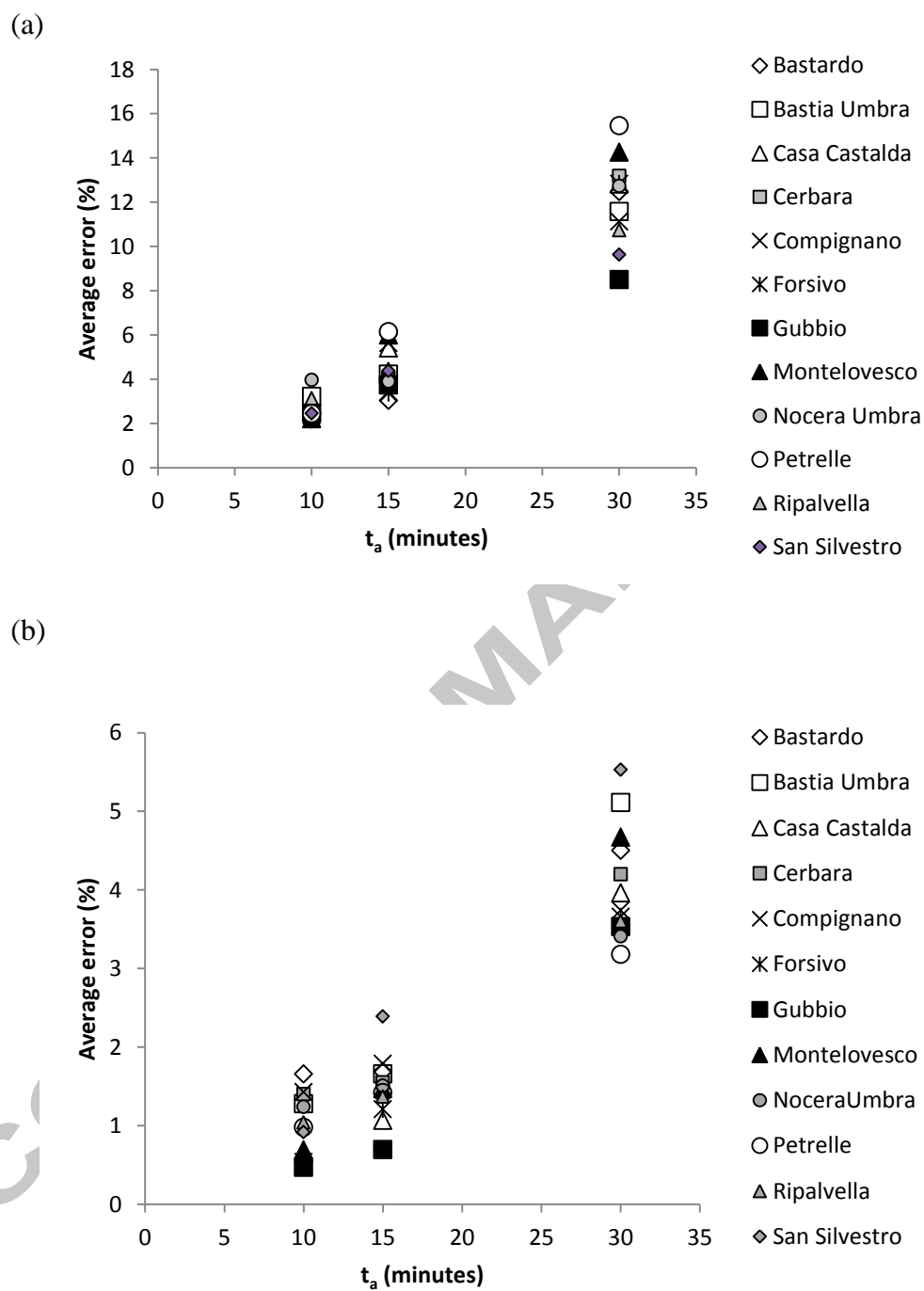


Fig. 6 – Average underestimation error of the annual maximum rainfall depth as a function of the aggregation time, t_a , for two different durations: (a) $d=30$ minutes; (b) $d=60$ minutes. Rainfall stations used during the first phase of this work.

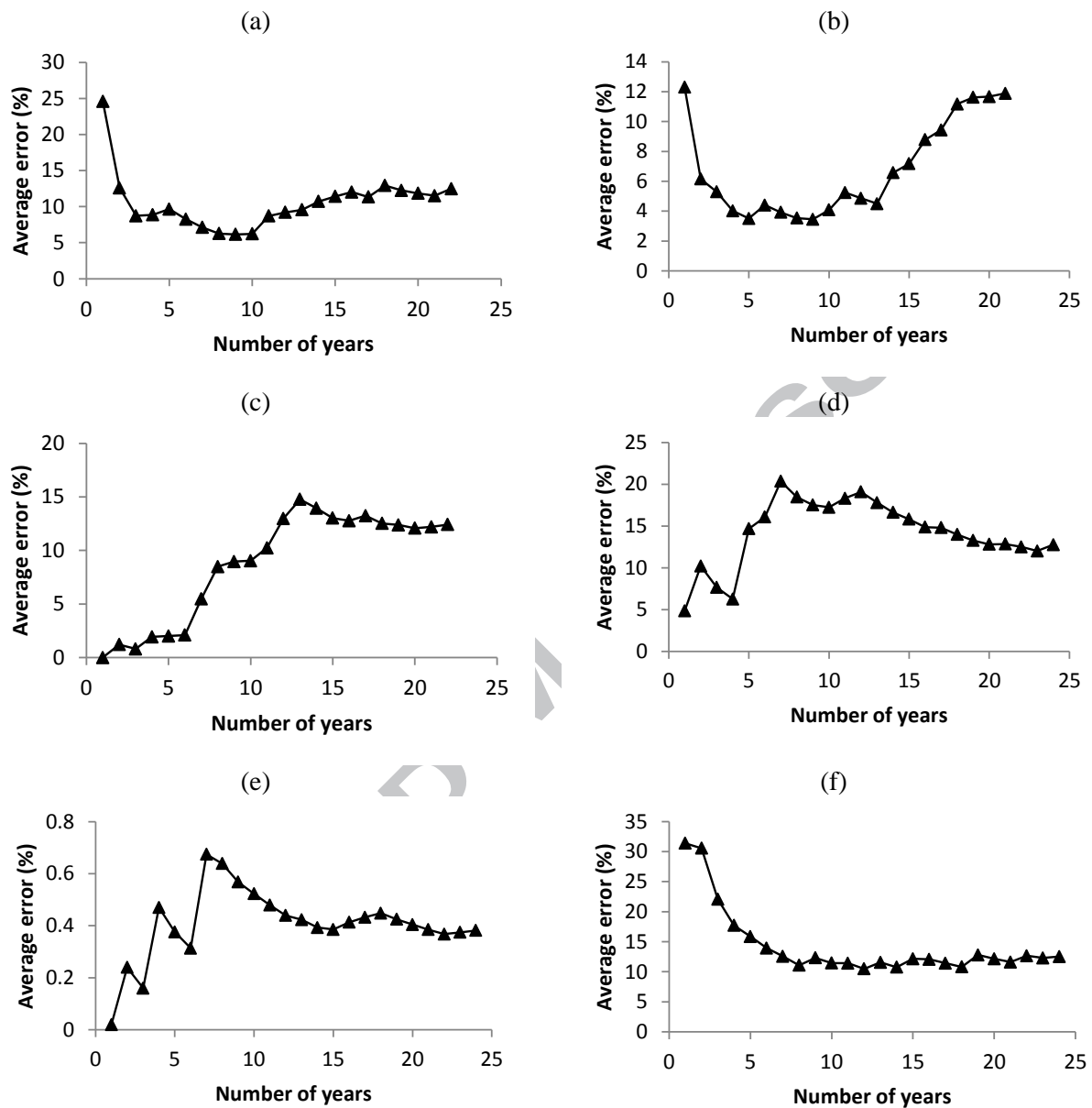


Fig. 7 – Average errors in the evaluation of annual maximum rainfall depth, H_d , as a function of the number of years preceding the last H_d value for different combinations of aggregation time, t_a (in minutes), and duration, d (in minutes): (a) Bastardo station, $t_a=30$, $d=30$; (b) Cerbara station, $t_a=30$, $d=30$; (c) Ponte Santa Maria station, $t_a=60$, $d=60$; (d) Ripalvella station, $t_a=60$, $d=60$; (e) Nocera Umbra station, $t_a=30$, $d=180$; (f) Nocera Umbra station, $t_a=30$, $d=30$.

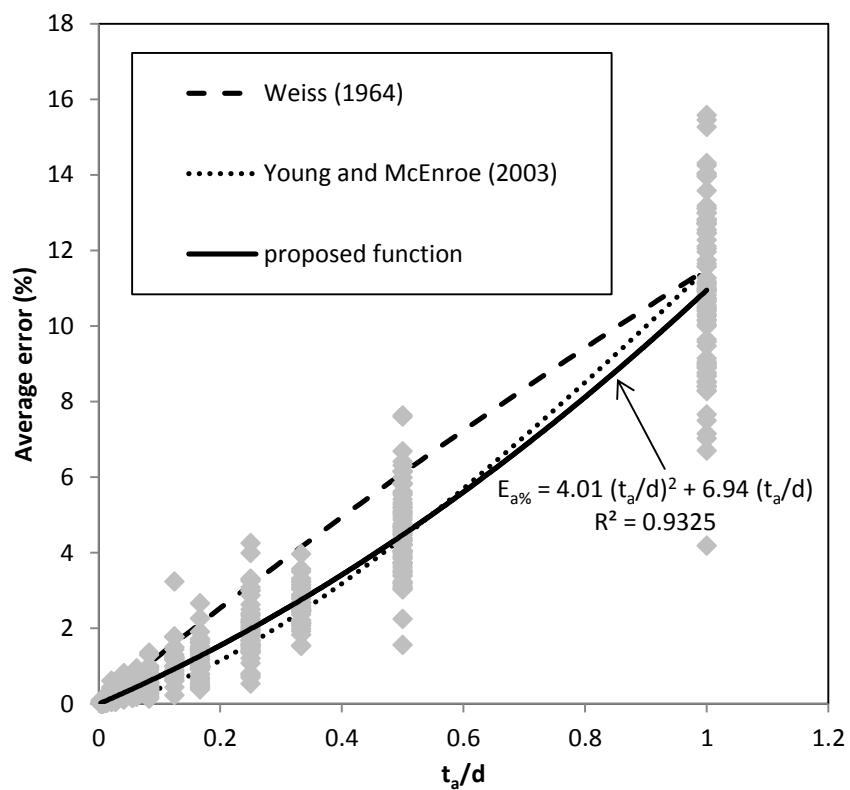


Fig. 8 – Average underestimation error of the annual maximum rainfall depth (\diamond) as a function of the ratio between temporal aggregation, t_a , and duration, d , for 12 rainfall stations used in the first phase of this work and all the combinations of t_a and d examined here. The best interpolating function together with the relations suggested by Weiss (1964) and Young and McEnroe (2003) are also plotted.

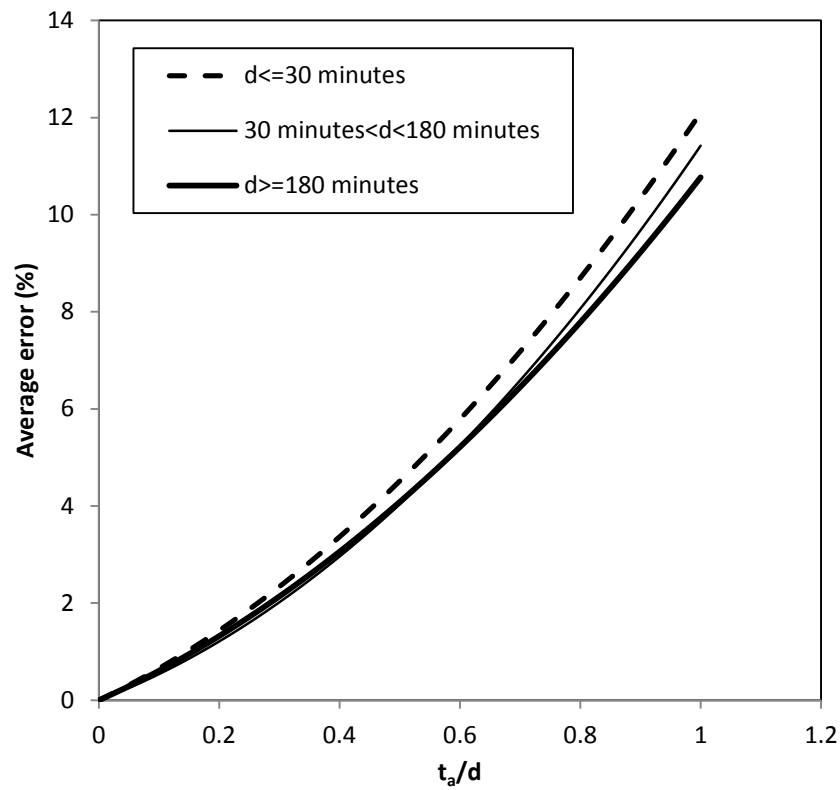


Fig. 9 - Average underestimation error of the annual maximum rainfall depth obtained by eq. (8) as a function of the ratio between aggregation time, t_a , and duration, d .

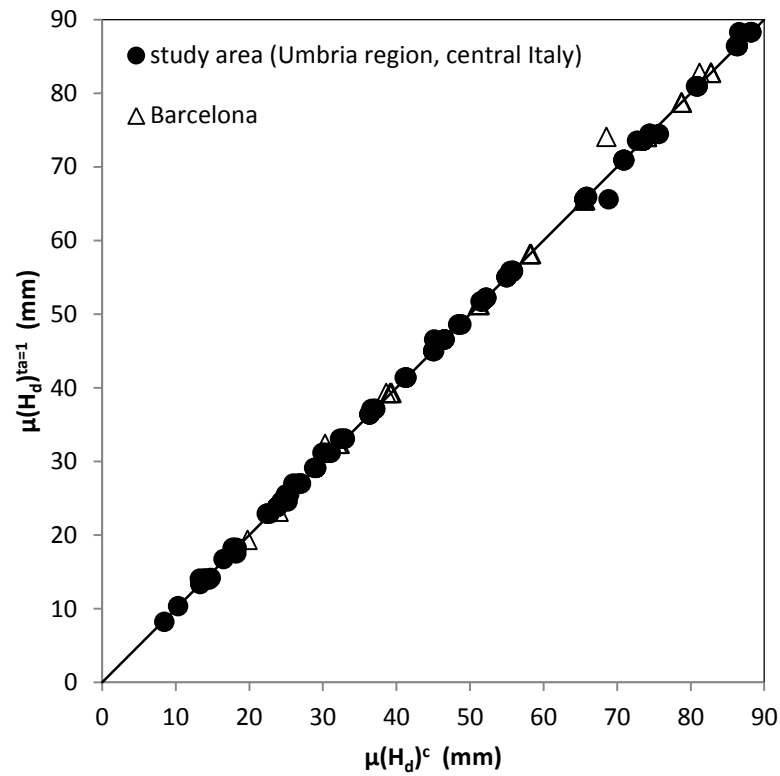


Fig. 10 – “Corrected” average annual maximum rainfall depths, $\mu(H_d)^c$, as a function of the corresponding values derived from rainfall data with $t_a=1$ minute, $\mu(H_d)^{t_a=1}$. Results from rain gauge stations selected for the validation phase.

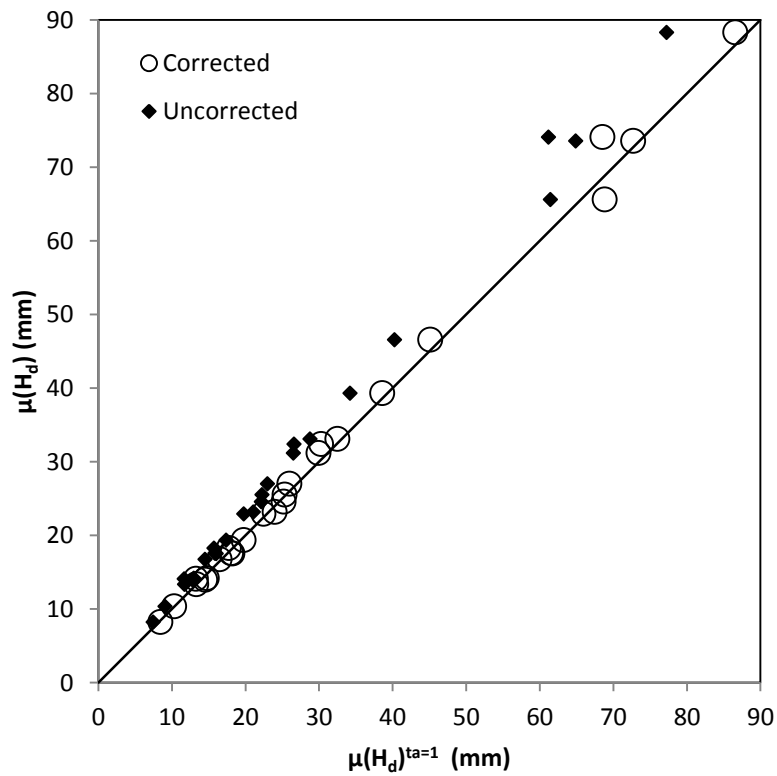


Fig. 11 – Average annual maximum rainfall depths, $\mu(H_d)$, versus the corresponding values derived from rainfall data with $t_a=1$ minute, $\mu(H_d)^{t_a=1}$. “Uncorrected” and “Corrected” stand for the values obtained before and after the application of the proposed methodology, respectively. Rainfall data from the stations used in the validation phase. Only cases with duration equal to the aggregation time are shown.

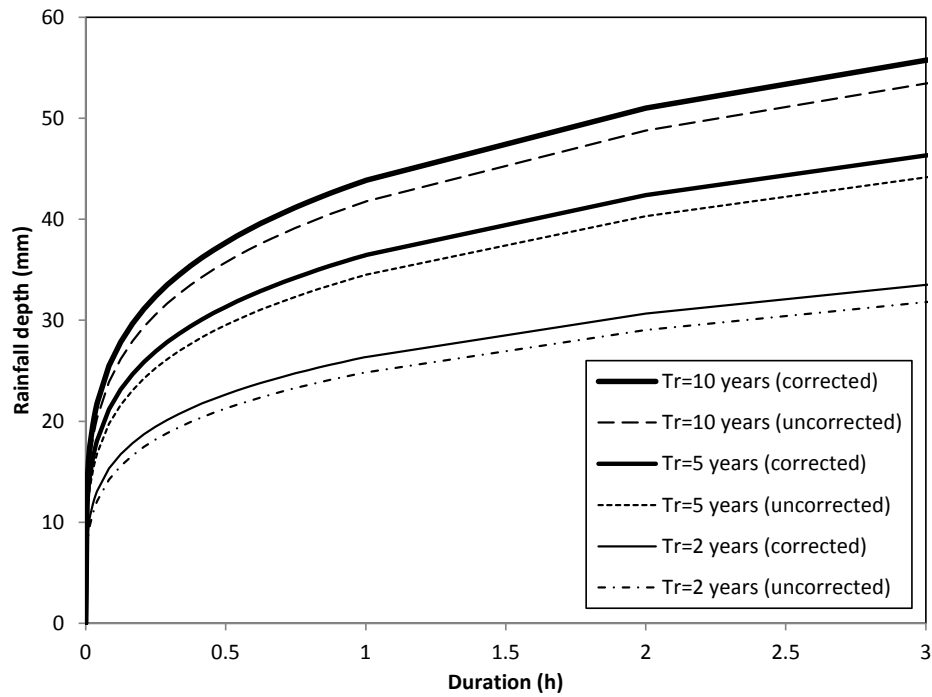


Fig. 12 – Rainfall depth-duration curves for different return periods, T_r . Comparison of curves obtained by uncorrected H_d series and corresponding series corrected by the proposed methodology. Sample rain gauge station of Gubbio.

653 **Highlights**

654

655 Rainfall data to be used in the hydrological practice is available in aggregated form

656

657 Aggregated form produce the underestimate of annual maximum rainfall depth (H_d)

659

Errors in the H_d evaluation from data with coarse time aggregations are investigated

660

661 Relationships to overcome the underestimate of H_d are presented

662

663

ACCEPTED MANUSCRIPT